CEAS - AIDAA Conference 2025 Materials Research Forum LLC
Materials Research Proceedings 69 (2026) 125-129 https://doi.org/10.21741/9781644904251-22

Computational Analysis to Improve the Aerodynamic Performance of NACA 0012 in Transonic Flow Using Raw Riblet Patterns

Siva MARIMUTHU[1,a *], Sheikh ISLAM[1,b], Parvathy RAJENDRAN[2,c], Rajadurai MURUGESAN[3,d]

[1]Department of Engineering, University of Staffordshire, Stoke on Trent, United Kingdom

[2]School of Aerospace Engineering, University Sains Malaysia, Seberang Perai, Malaysia

[3]Department of Aeronautical Engineering, Nitte Meenakshi Institute of Technology, Bengaluru, India

[a]siva.marimuthu@staffs.ac.uk, [b]sheikh.islam@staffs.ac.uk, [c]aeparvathy@usm.my, [c]mrajadurai700@gmail.com

Keywords: Computational Analysis, Viscous Drag, Raw-Riblets, Surface Pattern

Abstract. Emission reduction is of global importance and a big challenge in the aviation industry. In this research project, the emission issue was addressed aerodynamically by improving the performance of wings in transonic flow. This improvement was achieved by implementing a Raw-riblet pattern at different locations on the top surface of the wing as this showed higher values of viscous drag. Viscous drag is a large composition of total drag and reducing them will help to reduce the fuel consumption of aircraft and effectively reduce the carbon emissions. Two types of designs named Low-depth (0.305) and Low-depth (0.455) patterns were developed based on the 'Raw Riblet'. Computational analyses were carried out in the commercial code FLUENT with the help of the Spalart-Allmaras turbulence model to capture the viscous drag issues on the normal NACA 0012 wing at different angles of attack and solved them using the biomimetic patterns implemented. It was evidenced in this research work that the Low-depth (0.455) Raw Riblet pattern could reduce a significant amount of viscous drag on the NACA wing when compared to the Low-depth (0.305) pattern. Compatibility tests were done to check the suitability and stability of the model and mesh, respectively, and compared them to the experimental results. This research demonstrated the potential of surface texture-based solutions for aerodynamic design improvement and emission reduction.

Introduction

Commercial aviation has grown every year. Airbus has forecasted 43420 new aircraft deliveries between 2025 and 2044 [1]. This will increase aviation emissions in near future. Xueli et al., mentioned in their work that carbon emissions are a concern in the aviation industry [2]. Carbon emission from commercial aviation is expected to contribute 25% of overall emissions by 2050 [3]. It is essential that this issue needs to be addressed. Feuvre [4] stated that the aviation industry is committed to reducing carbon emissions by 50% in the year 2050. To mitigate this issue, a number of research are still carried out in the areas of propulsion, aerodynamics, structures, aircraft design and beyond. Capoccitti et al., [5] discussed about three important areas for researchers to look at in order to reduce the use of fossil fuels. They are structural (weight), propulsion (engine) and aerodynamic improvements. Out of these three elements, aerodynamic improvement was selected in this research project and it can be achieved by reducing drag on aircraft [6]. The longest phase of a commercial aircraft is the cruise and in that flight phase, the amount of skin-friction drag generation would be as high as 50% of total drag [7]. Skin friction drag, which is also known as viscous drag, is generated because of the contact (sliding motion, especially) between the aerodynamic body and air particles. Kumar et al., [8] reviewed five types of viscous drag reduction

Materials Research Proceedings 69 (2026) 125-129 https://doi.org/10.21741/9781644904251-22

methods and concluded that surface morphology is the most reliable method because it has been verified both computationally and experimentally. Liu et al., [9] proved in their research work that the surface structures could reduce the disturbances in the fluid flow. Lloyd et al., [10] mentioned in their research that shark-skin mimicked structures have evolved as a mechanism to reduce skin friction. The most common method used to develop a surface structure is biomimetics. In this method, the solutions are observed and mimicked from nature to solve the issues in engineering sciences. Our previous research works on shark skin inspired surface patterns had proved that a significant amount of drag reduction could be achieved in airflow [11-14]. Hence, in this research, the same 'Raw Riblet' pattern was implemented on the chosen wing surface (especially, where the issues identified) in different ways to reduce the skin friction drag, which is the main aim of this research.

Computational Design

Using the coordinates from airfoiltools.com [15], the NACA 0012 aerofoil was generated in the SolidWorks software and it was then extruded into a three-dimensional model, as shown in Fig. 1(a). In previous research work [11], the Raw Riblet (RR) pattern, which is shown in Fig. 1(b), was developed using the scanning microscopic image of a Requiem shark. This RR pattern was then implemented on the NACA 0012 wing surface in two different positions based on the issues observed. Fig. 1(c) depicts the implemented hollow RR pattern near the leading edge with a cut-depth of 0.455 metres from the top to mid-surface and hence, called a one low depth RR (1-LRR, 0.455) model. Similarly, another design was made by reducing the cut-depth from 0.455 to 0.305 metres for analysing the influence of depth in the performance of the RR pattern and hence, called the one lower depth RR (1-LRR, 0.305) model, which is shown in Fig. 1(d). All these designs were then exported to IGES format and imported into ANSYS.

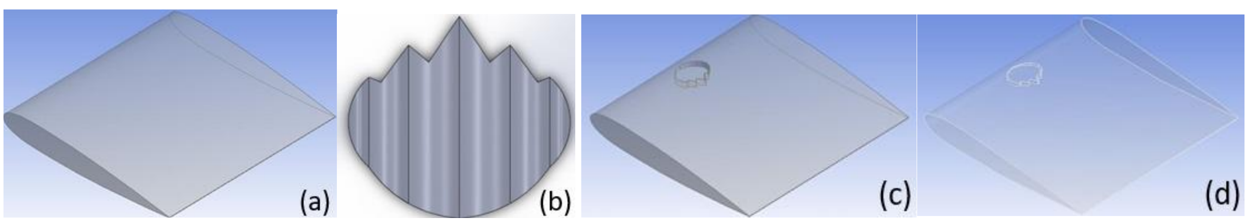

Figure 1. (a) NACA 0012, (b) Top view of RR[11], (c) 1-LRR (.455), (d) 1-LRR (0.305)

Computational Analysis

The three-dimensional NACA 0012 wing was imported into ANSYS Design Modeler and a computational domain was created. With the use of the Boolean tool, the solid boundary and wing were defined. This was then read into Mesh, where all the solid surfaces of the wing were named as top, bottom, trailing edge and riblets. The outer computational domain was considered the control volume, through which the air flows. Higher order elements and program-controlled automatic inflation were opted to minimise the errors and not inflate the selected boundaries, respectively. Most of the settings were set to default and the mesh was generated with 1.9 million nodes and 1.3 million elements. Quality check was carried out and the meshed design was brought into Fluent and the polyhedral mesh was selected, which helped reduce the element size, nodes and computational time. The Spalart-Allmaras viscous model was chosen as it involves the solution of the kinematic turbulent viscosity transport equation only, and it agrees well with experimental results [16]. Hence, less effort is required to solve when compared to other models. As the Eulerian approach was selected, the angle of flow was modified. A coupled solution method was chosen and discretization variables were defined as second order to reduce the time in solving the equations and then the iterations were done. These simulations were repeated for different angles of attack (0^0, 3^0, 6^0, 9^0, 12^0), in the 0.8 Mach number flow, which matched the cruise speed

Materials Research Proceedings 69 (2026) 125-129 https://doi.org/10.21741/9781644904251-22

of commercial flights in general. The same computational simulation procedure was repeated for 1-LRR (0.455) and 1-LRR(0.305) models.

Results and Discussion

Outputs such as lift coefficient and viscous drag values were noted at the end of analyses. Based on the comparison between the lift coefficient results, which is shown in Fig. 2(a), it was observed that both 1-LRR(0.455) and 1-LRR(0.305) had generated the same levels of lift at 3^0, 6^0, 9^0 and slightly lesser levels of lift at 0^0 and 12^0, when compared to the NACA 0012. These are acceptable levels and thus demonstrate potential in biomimetic designs. Similarly, comparing the viscous drag results against angle of attack, as shown in Fig. 2(b), it was identified that both biomimetic designs performed very well in reducing the drag when compared to the original wing at all of angles of attack. When the angle of attack was increased, the rate of viscous drag reduction was observed largely in both biomimetic designs.

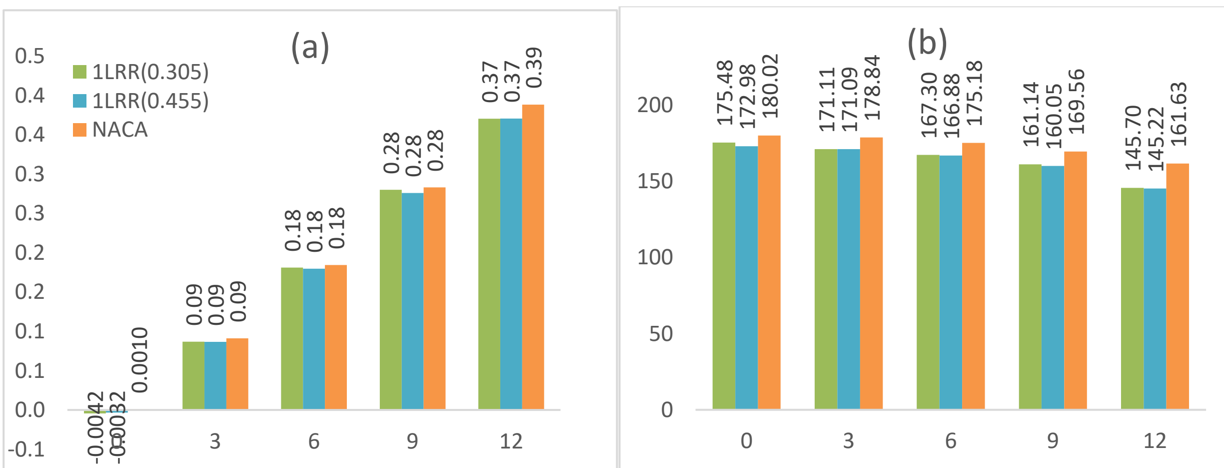

Figure 2. (a) Lift Coefficient Vs Angle of Attack, (b) Viscous Drag Vs Angle of Attack

1-LRR (0.455) reduced the viscous drag between the range 3.91 and 10.15 % from 0^0 to 12^0 angles of attack. Although 1-LRR(0.305) model has reduced the drag in the range of 2.52 to 9.85%, it is still a bit less than the deeper 1-LRR (0.455) model. For example, at 12^0 angle of attack, NACA 0012's top surface has medium and low values of skin friction drag as shown in Fig. 3(a). This is higher when compared to both biomimetic designs. Fig. 3(b) and (c) illustrate the skin friction contours of 1-LRR(0.455) and 1-LRR(0.305), respectively. From these figures, it can be noted that the skin friction distribution values on 1-LRR(0.455) were much lower compared to those on 1-LRR(0.305). This is due to the differences in the depths of the hollow raw riblet patterns applied on the models. The hollow pattern enabled the reversed flow at high angles of attack to circulate, lift, re-reverse/straighten and join the mainstream flow. This reduced the disturbance in the flow, which led to a reduction in the skin-friction coefficient.

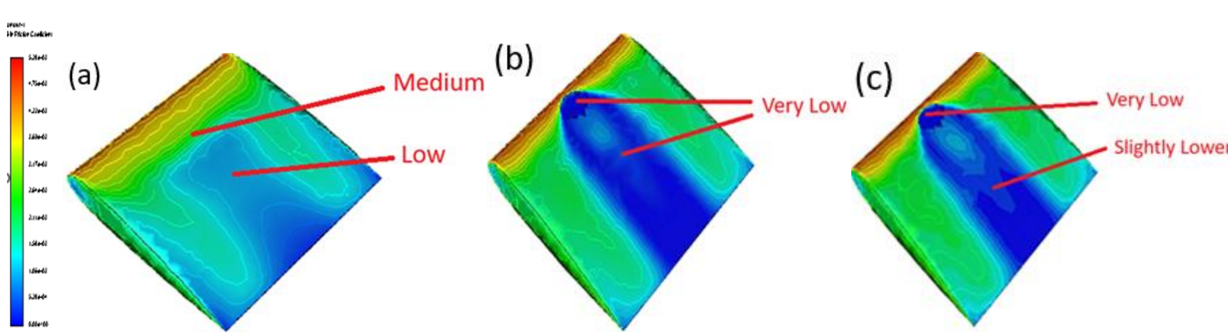

Figure 3. Skin Friction Contour at 12^0: (a) NACA 0012, (b) 1-LRR (0.455), (c) 1-LRR (0.305)

Validation

Validation tests were carried out to verify the accuracy of the procedure and results. In the model compatibility test, many viscous models such as K-epsilon, K-omega, Transition K-Kl-omega and Spalart Allmaras were used to analyse the NACA 0012, separately, to find a suitable turbulence model for this research. Eventually, the Spalart Allmaras was selected as it resulted in closer agreement with experimental values. In order to find a suitable mesh, a grid compatibility test was conducted. This was done by meshing the NACA 0012 model with their control volume at different mesh element sizes, such as 0.3, 0.4, 0.5, 0.6, 0.7, 0.8, 0.9, 1, 1.5 and 2 and solving them in Fluent. Additionally, a grid independence test was carried out to ensure the stability of the results. Based on these tests, a 0.5 mesh element size was chosen as it agreed well with the experimental values and had used them the mesh procedure.

Conclusion

As aimed, the viscous drag reduction was achieved in both models using the biomimetic pattern. Especially, the 1-LRR(0.455) model achieved a maximum of 10.15% viscous drag reduction at 120 angle of attack in the transonic flow regime. This aerodynamic improvement would help reduce the fuel consumption requirements and hence, emissions. Overall, this research has proved the potential in the hollow biomimetic raw riblet pattern in reducing the viscous drag and improving the wing aerodynamics. Technical elements such as structural strength of the wing, experimental modelling and tests are to be explored in the future for further enhancement of this work and bringing this idea into reality.

References

[1] Information on https://www.airbus.com/en/products-services/commercial-aircraft/global-market-forecast.

[2] Xiong, X., Song, X., Kaygorodova, A., Ding, X., Guo, L. and Huang, J., Aviation and carbon emissions: Evidence from airport operations, Journal of Air Transport Management, 109, p.102383, (2023), https://doi.org/10.1016/j.jairtraman.2023.102383

[3] Graver, B., and Zhang, K., CO2 emissions from commercial aviation 2018, The International Council on Clean Transportation, pp. 1- 13, (2019).

[4] Feuvre, P.L., Are aviation biofuel is ready for take off?, (2019), https://www.iea.org/commentaries/are-aviation-biofuels-ready-for-take-off.

[5] Capoccitti, S., Khare, A., and Mildenberger, U., Aviation industry - mitigating climate change impacts through technology and policy, Journal of Technology Management and Innovation, pp. 66-75, (2010).

[6] Nath, D.S., Pujari, P.C., Jain, A. et al., Drag reduction by application of aerodynamic devices in a race car, Advances in Aerodynamics, 3, 4 (2021), https://doi.org/10.1186/s42774-020-00054-7.

[7] Ricco, P., Stoke, M., and Leschziner, M.A., A review of turbulent skin-friction drag reduction by near-wall transverse forcing, Progress in aerospace sciences, pp.1-137, (2021).

[8] Kumar, S., Pandey, K.M., and Sharma, K.K., Advances in drag-reduction methods related with boundary layer control – A review, Materials Today: Proceedings 45, pp. 6694-6701, (2021).

[9] Liu, Q., Zhong, S., and Li, L., Effects of Bio-inspired micro-scale surface patterns on the profile losses in a linear cascade, Journal of Turbomachinery, 141(12): 121006, (2019).

Materials Research Proceedings 69 (2026) 125-129 https://doi.org/10.21741/9781644904251-22

[10] Lloyd, C.J., Peakall, J., Burns, A.D., Keevil, G.M., Dorrell, R.M., Wignall, P.B., and Fletcher T.M., Hydrodynamic efficiency in sharks: the combined role of riblets and denticles, Bioinspiration and Biomimetics, 16 (4), pp. 1-17, (2021).

[11] Marimuthu, S., and Chinnathambi, D., Computational analysis of biomimetic butterfly valve, Bioinspired, Biomimetic and Nanobiomaterials, 9 (4): 223–232, (2020), https://doi.org/10.1680/jbibn.20.00027.

[12] Marimuthu, S., Natarajan, S., Ramesh R., and Murugesan, R., Hollow Three-dimensional Model for Fuel Reduction in Aviation Industry, International Journal on Interactive Design and Manufacturing, (2022), https://doi.org/10.1007/s12008-022-00883-4.

[13] Marimuthu, S., Al-Rabeei, S., and Boha, H-A., Three-dimensional analysis of biomimetic aerofoil in transonic flow, Biomimetics (MDPI), 7(1), 20, (2022), https://doi.org/10.3390/biomimetics7010020.

[14] Marimuthu, S., and Chinnathambi, D., Computational Analysis to Enhance the Compressible Flow over an Aerofoil surface, Aircraft Engineering and Aerospace Technology, 93(5), 925-934, (2021), https://doi.org/10.3390/biomimetics7010020.

[15] Information on http://airfoiltools.com/.

[16] Pellerin, N., Leclaire, S., and Reggio, M., An implementation of the Spalart–Allmaras turbulence model in a multi-domain lattice Boltzmann method for solving turbulent airfoil flows. Computers & Mathematics with Applications, 70(12), pp.3001–3018, (2015), https://doi.org/10.1016/j.camwa.2015.10.006.